

Results from IceCube Follow-up of Nearby Supernova SN2023ixf

The IceCube Collaboration

(a complete list of authors can be found at the end of the proceedings)

E-mail: aemand@wisc.edu, justin.vandenbroucke@wisc.edu,
jessie.thwaites@icecube.wisc.edu, sahori@icecube.wisc.edu,
aswathi.balagopalv@icecube.wisc.edu

Core-collapse supernovae are of particular interest in multi-messenger astronomy due to their potential to accelerate cosmic rays and produce high-energy neutrinos. One such supernova is the recent SN2023ixf located in M101 (the Pinwheel Galaxy). It is the closest (6.4 Mpc) and brightest (B band magnitude 10.8) core-collapse supernova in nearly a decade. This supernova likely had a progenitor surrounded by dense circumstellar material which, during the supernova, may have produced neutrinos when ejecta collided with the material. I will present results of a follow-up of this supernova using data collected from the IceCube Neutrino Observatory located at the South Pole. We obtain results consistent with background expectations with time-integrated energy flux ($E^2 \text{ dN/dE}$) upper limits of 0.35 GeV/cm^2 for a 32-day time window and 0.44 GeV/cm^2 for a 4-day time window, both at 90% confidence level for an E^{-2} power law. These correspond to values of $2.7 \times 10^{48} \text{ erg}$ for the 32-day time window and $3.5 \times 10^{48} \text{ erg}$ for the 4-day time window at the supernova.

Corresponding authors: Alicia Mand^{1*}, Justin Vandenbroucke¹, Jessie Thwaites¹, Sam Hori¹, Aswathi Balagopal V²

¹ *Dept. of Physics and Wisconsin IceCube Particle Astrophysics Center, University of Wisconsin—Madison*

² *University of Delaware*

* Presenter

39th International Cosmic Ray Conference (ICRC2025)
15–24 July 2025
Geneva, Switzerland



1. Introduction

Multi-messenger astronomy is a powerful tool for probing extreme astrophysical phenomena in new ways. By combining information from neutrinos and optical observations, we can examine high-energy transients with a new lens. One example of these transients are type-II core-collapse supernovae which produce optical light and are expected to produce high-energy neutrinos [1].

Supernova 2023ixf (hereafter, SN 2023ixf) is a type-II core-collapse supernova discovered on May 19, 2023 by K. Itagaki. It is located in M101 (the pinwheel galaxy) at a distance of 6.4 Mpc at RA, Dec. = 210.9°, 54.3° and is the closest and brightest supernova in nearly a decade [2]. Several observatories, including the IceCube Neutrino Observatory, performed rapid follow-ups after the initial detection [3].

We describe a search for neutrinos coincident with SN 2023ixf using IceCube's Northern Tracks data sample and kernel density estimator method (KDEs) for improved energy and angular reconstruction [4]. Section 2 describes the IceCube Neutrino Observatory and the data selection used in this analysis. Section 3 discusses models for neutrino production from SN 2023ixf, and section 4 discusses our search for neutrinos from the supernova. Finally, in section 5 we provide a discussion of this search as well as a comparison of previous IceCube supernova analyses.

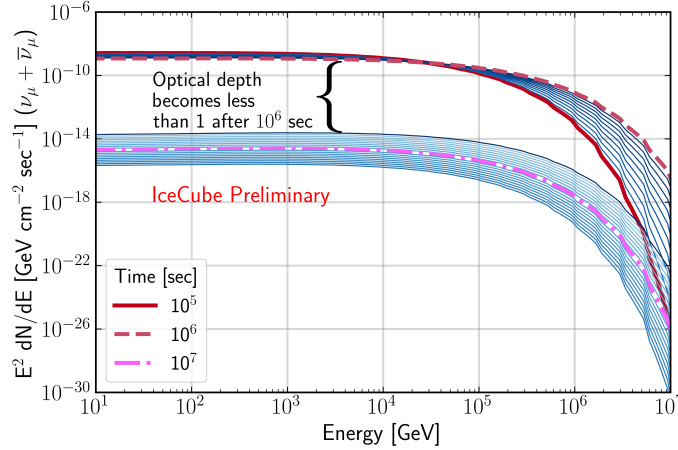


Figure 1: Time evolution of predicted neutrino flux from SN 2023ixf according to [5]. After approximately 10^6 seconds, the optical depth becomes less than 1, significantly reducing the flux. The blue lines correspond to different instances in time with spacing of 10 lines per decade. At high energies, the availability of simulation decreases per energy decade, resulting in the "wiggle" features [6].

2. Models for Neutrino Production

During the gravitational collapse of the core of a massive star ($M_* > 8M_\odot$) during a type-II supernova, most of the gravitational binding energy is converted into thermal neutrinos with energies on the order of tens of MeV. In addition to these neutrinos, supernova progenitors surrounded by dense circumstellar material (CSM) have been predicted to produce high-energy neutrinos. Specifically, supernova ejecta interacts with the CSM and acts as a proton accelerator through diffusive shock acceleration. The accelerated protons interact with other protons present in the

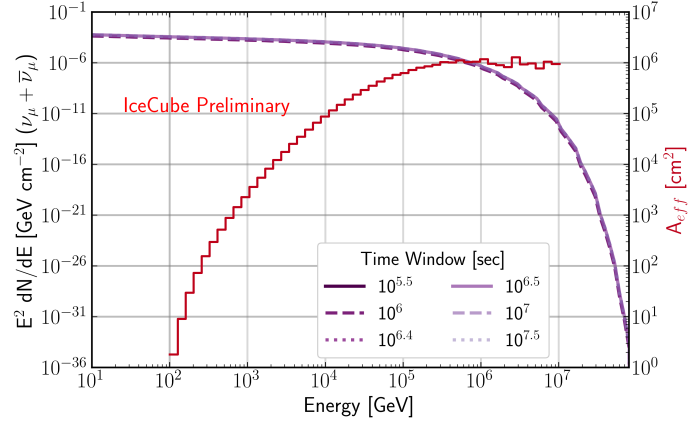


Figure 2: Effective area of IceCube (red) as a function of neutrino energy (for $\nu_\mu + \bar{\nu}_\mu$) with modeled time-integrated flux from [5]. In this figure, all of the purple lines lie on top of one another.

CSM and produce high-energy neutrinos via the p-p interaction. These neutrinos, which can have energies of up to TeV scale, would be detectable by IceCube [5, 7–9].

In order to motivate our analysis, we examine the model presented in [5] for neutrino production in SN 2023ixf through proton acceleration in CSM. In this model, neutrino flux is a function of the time after the supernova explosion. After a time period of approximately 10^6 seconds, neutrino production slows down as the optical depth becomes less than 1, which is shown in Figure 1.

We can use this model to calculate the expected number of neutrinos detectable by IceCube by combining IceCube’s effective area with the neutrino flux to produce expected neutrinos as a function of time after supernova explosion as seen in figure 2. The total time that we observe the supernova for is called a time-window. For a plot of the expected number of neutrinos as a function of time post-explosion, see Figure 3.

3. Neutrinos with IceCube

The IceCube Neutrino Observatory is a cubic kilometer neutrino detector located at the geographic South Pole consisting of 86 strings with a total of 5160 digital optical modules (DOMs). These DOMs are situated between 1.5 km and 2.5 km below the glacial surface in a hexagonal grid and are optimized for the detection of high-energy (TeV - PeV) neutrinos [10]. The DOMs consist of 10-inch photomultiplier tubes encased in a pressurized glass housing for detecting Cherenkov emission from secondary charged particles from the interaction of neutrinos in the Antarctic ice. Neutrino detections result in two topologies of events: tracks and cascades. Charged current ν_μ interactions product a track-like signature from the secondary muon that can travel up to several kilometers through the ice depending on the energy. All other neutrino interactions produce a near-isotropic light distribution in the detector called a cascade. Track-like signatures have an angular resolution of $\sim 1^\circ$ and cascades have a worse resolution of $\sim 10^\circ$.

For our analysis, we use the Northern Tracks data sample which contains track events in a declination range of $-5^\circ < \delta < 90^\circ$ and boasts a livetime of 13.5 years covering the period 06/01/2010 - 11/28/2023 (which includes the supernova discovery time). We select this event sample

because our target declination ($\delta = 54.3^\circ$) is located in the northern hemisphere and Northern Tracks is the most sensitive dataset for the search of point sources in the northern hemisphere. Finally, kernel distribution estimators (KDEs) are implemented for the probability density functions (PDFs), which improves sensitivity by replacing the usual Gaussian approximation for the spatial PDF by a non-parametric inference of the same PDF [4].

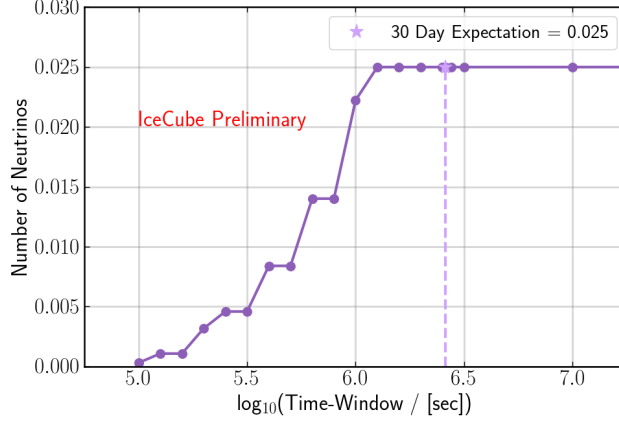


Figure 3: Model expectation of neutrinos detected by IceCube from SN 2023ixf as a function of time after supernova explosion. There is no significant increase in neutrinos after approximately $10^{6.1}$ sec. Our selected time-window of 30 days post-explosion has been marked with a star – which has an expectation of 0.025 detected neutrinos. The step behavior is a feature of the time binning in the model presented in [5].

4. Follow-up

IceCube’s realtime response of SN 2023ixf consisted of a 4-day time-window centered around the discovery time of the transient using IceCube’s Gamma-ray Follow-Up (GFU) event sample for muon neutrinos above 100 GeV in energy. GFU is IceCube’s online event sample and is used in realtime and fast response analyses (FRAs) [11]. IceCube obtained results consistent with background expectation and set time-integrated flux upper limits ($E^2 \text{ dN/dE}$) of $7.3 \times 10^{-2} \text{ GeV cm}^{-2}$ assuming an E^{-2} spectrum [3]. The zoomed-in skymap for the fast response analysis can be seen in Figure 4.

Using the model [5] discussed in section 2 and the sensitivities of IceCube, we estimate the expected number of neutrinos for various time-windows in order to optimize our analysis. We see that after 30 days, there is not a significant increase in the number of expected neutrinos from SN 2023ixf (see Figure 5). As a result, we are motivated to optimize our analysis for 30-days post discovery time. Using forced photometry data taken by the Zwicky Transient Facility (ZTF) to capture the last observation of SN 2023ixf pre-discovery, we include 2 additional days in our time window, prior to SN 2023ixf’s discovery, in order to capture the explosion time. This gives us a total time-window of 32-days, with 2 days prior to discovery and 30 days post-discovery.

We then construct a test statistic distribution using the following definition:

$$\text{TS} = -2n_s + 2 \sum_{i=1}^N \log \left[1 + \frac{n_s S(\mathbf{x}_i, \mathbf{x}_s)}{n_b B(\mathbf{x}_i)} \right], \quad (1)$$

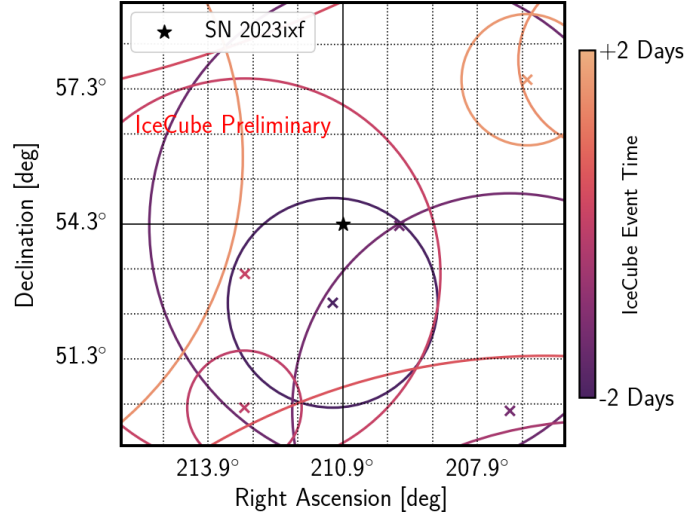


Figure 4: Fast response analysis zoomed-in skymap at the location of SN 2023ixf for a 4 day time window centered at ZTF discovery time. This depicts on-time events within ± 10 degrees of the target location in both RA and dec. IceCube obtained a p-value of 0.18, consistent with background expectation and an upper limit of $E^2 dN/dE = 7.3 \times 10^{-2} \text{ GeV cm}^{-2}$ at 90%CL for energy range between 600 GeV and 250 TeV. Here, the size of each circle corresponds to the angular uncertainty (90%) for each neutrino.

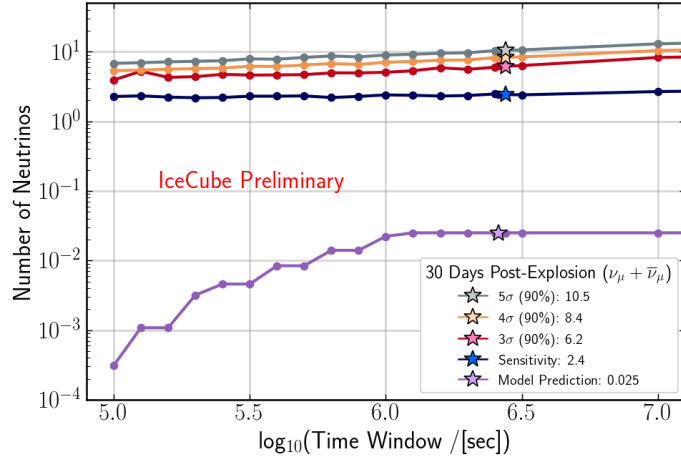


Figure 5: Sensitivity, 3σ , 4σ , 5σ , and model expectation (taken from [5]) as a function of time-window. Target time window of 30 days post-explosion has been marked with a star for each line. This plot is for $\nu_\mu + \bar{\nu}_\mu$ only.

where n_s is the fitted number of signal events, \mathbf{x}_i are the reconstructed properties of IceCube neutrino candidates, \mathbf{x}_s is the location on the sky of the tested source position, S is the signal probability density function (PDF), B is the background PDF, n_b is the expected number of background events, and N is the total number of events in the event selection. This equation includes a Poisson term, which compares the total number of observed neutrinos in a time-window with the number expected from background. We then maximize this test statistic only using events that occur within our selected time window of 32 days the model prediction and estimation of the explosion time

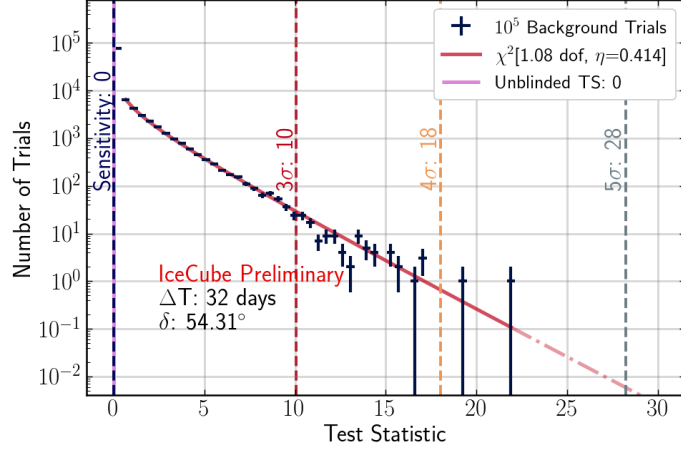


Figure 6: Test statistic distribution for SN 2023ixf at a time-window of 32 days, of which, 2 days are prior to discovery of the supernova. Unblinded TS of 0 is shown at the left side of the plot in a solid pink line, additionally we show the sensitivity of IceCube at the declination of SN 2023ixf and the 3σ , 4σ , and 5σ potentials. Here η is the fraction of trials outside the 0 bin. At a TS of approximately 21, we no longer have background trials to fit χ^2 to. We represent this extrapolation of the χ^2 fit as a dash-dot line. For short time windows, if $\eta < 5$, more than half of the background trials are in the TS = 0 bin, resulting in a median value of 0. Since we define our sensitivity as the number of neutrinos that result in 90% of pseudoexperiments exceeding the median, our sensitivity TS is also 0.

from the optical light curve. For our analysis, we use a signal PDF which includes an energy PDF. For the energy PDF we assume that neutrino emission follows a power-law spectrum with an index of 2.0 to match the model presented in [5].

We calculate a test statistic distribution assuming a background only hypothesis. This is done by performing 10^5 pseudoexperiments of data at our target declination that has been randomly shuffled in RA [12]. For each pseudoexperiment, we calculate the test statistic and combine all of them into a single test statistic distribution comprised of background-only. When we unblind our analysis, we can calculate the test statistic of our signal to obtain a signal test statistic. Comparing this to our background test statistic gives us the significance of our signal. A figure showing our background test statistic distribution in addition to our unblinded signal test statistic, sensitivity, and various levels of significance are given in Figure 6.

5. Results and Discussion

We present the results of a 32 day follow-up of SN 2023ixf. We obtain values consistent with background expectation and set strong upper-limits on the neutrino flux of a type-II core-collapse supernovae at our target declination of 0.06 GeV cm^{-2} . This limit represents the strongest limit on the high-energy neutrino flux from core-collapse SNe obtained using IceCube data. We present and summarize limits from 3 IceCube analyses, including this one, and set the strongest limits thus far for supernovae. Our results are summarized in Table 1. These analyses include the initial realtime response to SN 2023ixf which encompasses a 4-day time-window centered at the supernova’s discovery time, this analysis which uses a 32 day time-window with 2 days prior to

discovery time and 30 days after, and finally, a stacking search for high-energy neutrino emission from core-collapse supernovae using IceCube data [3, 13]. Additionally, we plot our upper limits and model expectation in Figure 7.

Analysis	Upper-Limits (GeV cm^{-2})
SN 2023ixf Follow-up (this work)	0.06
Supernova Stacking Paper [13]	0.17
SN 2023ixf 4-Day Follow-up [3]	0.07

Table 1: Results from IceCube Supernovae Analysis

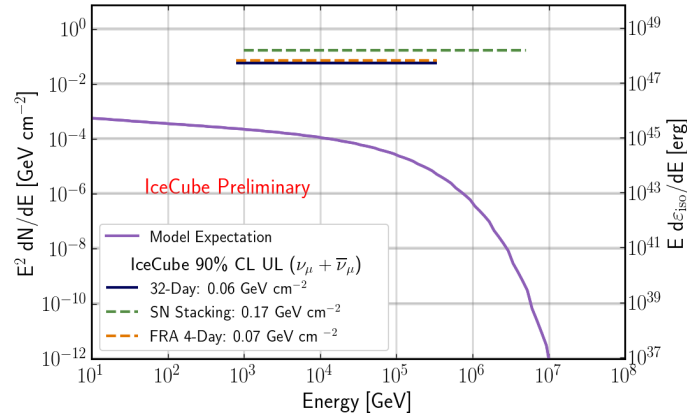


Figure 7: Upper limits from IceCube for SN 2023ixf. Included in this plot is the model expectation from [5] (purple), this analysis (dark blue), a previous IceCube Supernova Stacking analysis (green) [13], and the original IceCube SN 2023ixf Fast Response Analysis (orange) [3]. Here, the SN stacking line has been scaled for the distance to SN 2023ixf (distance = 6.4 Mpc) in order to make it more comparable to SN 2023ixf. The right axis shows the differential isotropic equivalent energy obtained with the expression: $E \frac{d\epsilon_{iso}}{dE} = \phi \frac{4\pi d_L^2}{1+z}$ where $\phi = E^2 dN/dE$ and the appropriate unit conversions have been applied.

We expect long-term improvements to neutrino detection using the IceCube Neutrino Observatory with the implementation of the IceCube Upgrade, currently being installed at the South Pole. The IceCube Upgrade will extend IceCube’s neutrino sensitivity to even lower energies (GeV and below) by increasing the density of the infill array’s (IceCube DeepCore) strings [14]. On a more long-term timescale, IceCube Gen-2 will provide increased instrument volume and the addition of Gen-2 Radio which, when combined, will extend improved sensitivity to the TeV-PeV energy range for high-energy neutrino emission from nearby supernovae [15].

References

- [1] D. Guetta, A. Langella, S. Gagliardini, and M. D. Valle, *The Astrophysical Journal Letters* **955** no. 1, L9. Publisher: The American Astronomical Society.
- [2] K. Itagaki, *Transient Name Server Discovery Report* **2023-1158** (May, 2023) 1.

- [3] J. Thwaites, J. Vandenbroucke, M. Santander, and IceCube Collaboration, *The Astronomer's Telegram* **16043** (May, 2023) 1.
- [4] **IceCube** Collaboration, C. Bellenghi, *PoS ICRC2023* (2023) 1060.
- [5] A. Kheirandish and K. Murase, *The Astrophysical Journal Letters* **956** no. 1, L8.
- [6] K. Murase, *Phys. Rev. D* **97** (Apr, 2018) 081301.
- [7] V. N. Zirakashvili and V. S. Ptuskin, *Astroparticle Physics* **78** 28–34.
- [8] P. Sarmah *et al.*, *Journal of Cosmology and Astroparticle Physics* **2022** no. 8, 011.
- [9] T. Pitik, I. Tamborra, M. Lincetto, and A. Franckowiak, *Monthly Notices of the Royal Astronomical Society* **524** no. 3, 3366–3384.
- [10] **IceCube** Collaboration, M. G. Aartsen *et al.*, *JINST* **12** no. 03, (2017) P03012.
- [11] **IceCube** Collaboration, R. Abbasi *et al.*, *The Astrophysical Journal* **910** no. 1, 4.
- [12] D. E. Alexandreas *et al.*, *Nuclear Instruments and Methods in Physics Research A* **328** no. 3, (May, 1993) 570–577.
- [13] **IceCube** Collaboration, R. Abbasi *et al.*, *The Astrophysical Journal Letters* **949** no. 1, L12.
- [14] **IceCube** Collaboration, A. Ishihara, *PoS ICRC2019* (2019) 1031.
- [15] **IceCube-Gen2** Collaboration, M. G. Aartsen *et al.*, *J. Phys. G* **48** no. 6, (2021) 060501.

Full Author List: IceCube Collaboration

R. Abbasi¹⁶, M. Ackermann⁶³, J. Adams¹⁷, S. K. Agarwalla^{39, a}, J. A. Aguilar¹⁰, M. Ahlers²¹, J.M. Alameddine²², S. Ali³⁵, N. M. Amin⁴³, K. Andeen⁴¹, C. Argüelles¹³, Y. Ashida⁵², S. Athanasiadou⁶³, S. N. Axani⁴³, R. Babu²³, X. Bai⁴⁹, J. Baines-Holmes³⁹, A. Balagopal V.^{39, 43}, S. W. Barwick²⁹, S. Bash²⁶, V. Basu⁵², R. Bay⁶, J. J. Beatty^{19, 20}, J. Becker Tjus^{9, b}, P. Behrens¹, J. Beise⁶¹, C. Bellenghi²⁶, B. Benkel⁶³, S. BenZvi⁵¹, D. Berley¹⁸, E. Bernardini^{47, c}, D. Z. Besson³⁵, E. Blaufuss¹⁸, L. Bloom⁵⁸, S. Blot⁶³, I. Bodo³⁹, F. Bontempo³⁰, J. Y. Book Motzkin¹³, C. Boscolo Meneguolo^{47, c}, S. Böser⁴⁰, O. Botner⁶¹, J. Böttcher¹, J. Braun³⁹, B. Brinson⁴, Z. Brisson-Tsavoussis³², R. T. Burley², D. Butterfield³⁹, M. A. Campana⁴⁸, K. Carloni¹³, J. Carpio^{33, 34}, S. Chattopadhyay^{39, a}, N. Chau¹⁰, Z. Chen⁵⁵, D. Chirkin³⁹, S. Choi⁵², B. A. Clark¹⁸, A. Coleman⁶¹, P. Coleman¹, G. H. Collin¹⁴, D. A. Coloma Borja⁴⁷, A. Connolly^{19, 20}, J. M. Conrad¹⁴, R. Corley⁵², D. F. Cowen^{59, 60}, C. De Clercq¹¹, J. J. DeLaunay⁵⁹, D. Delgado¹³, T. Delmeulle¹⁰, S. Deng¹, P. Desiati³⁹, K. D. de Vries¹¹, G. de Wasseige³⁶, T. DeYoung²³, J. C. Díaz-Vélez³⁹, S. DiKerby²³, M. Dittmer⁴², A. Domi²⁵, L. Draper⁵², L. Dueser¹, D. Durnford²⁴, K. Dutta⁴⁰, M. A. DuVernois³⁹, T. Ehrhardt⁴⁰, L. Eidenschink²⁶, A. Eimer²⁵, P. Eller²⁶, E. Ellinger⁶², D. Elsässer²², R. Engel^{30, 31}, H. Erpenbeck³⁹, W. Esmail⁴², S. Eulig¹³, J. Evans¹⁸, P. A. Evenson⁴³, K. L. Fan¹⁸, K. Fang³⁹, K. Farrag¹⁵, A. R. Fazely⁵, A. Fedynitch⁵⁷, N. Feigl⁸, C. Finley⁵⁴, L. Fischer⁶³, D. Fox⁵⁹, A. Franckowiak⁹, S. Fukami⁶³, P. Fürst¹, J. Gallagher³⁸, E. Ganster¹, A. Garcia¹³, M. Garcia⁴³, G. Garg^{39, a}, E. Genton^{13, 36}, L. Gerhardt⁷, A. Ghadimi⁵⁸, C. Glaser⁶¹, T. Glüsenkamp⁶¹, J. G. Gonzalez⁴³, S. Goswami^{33, 34}, A. Granados²³, D. Grant¹², S. J. Gray¹⁸, S. Griffin³⁹, S. Griswold⁵¹, K. M. Groth²¹, D. Guevel³⁹, C. Günther¹, P. Gutjahr²², C. Ha⁵³, C. Haack²⁵, A. Hallgren⁶¹, L. Halve¹, F. Halzen³⁹, L. Hamacher¹, M. Ha Minh²⁶, M. Handt¹, K. Hanson³⁹, J. Hardin¹⁴, A. A. Harnisch²³, P. Hatch³², A. Haungs³⁰, J. Häußler¹, K. Helbing⁶², J. Hellrung⁹, B. Henke²³, L. Hennig²⁵, F. Henningsen¹², L. Heuermann¹, R. Hewett¹⁷, N. Heyer⁶¹, S. Hickford⁶², A. Hidvegi⁵⁴, C. Hill¹⁵, G. C. Hill², R. Hmaid¹⁵, K. D. Hoffman¹⁸, D. Hooper³⁹, S. Hori³⁹, K. Hoshina^{39, d}, M. Hostert¹³, W. Hou³⁰, T. Huber³⁰, K. Hultqvist⁵⁴, K. Hymon^{22, 57}, A. Ishihara¹⁵, W. Iwakiri¹⁵, M. Jacquart²¹, S. Jain³⁹, O. Janik²⁵, M. Jansson³⁶, M. Jeong⁵², M. Jin¹³, N. Kamp¹³, D. Kang³⁰, W. Kang⁴⁸, X. Kang⁴⁸, A. Kappes⁴², L. Kardum²², T. Karg⁶³, M. Karl²⁶, A. Karle³⁹, A. Katil²⁴, M. Kauer³⁹, J. L. Kelley³⁹, M. Khanal⁵², A. Khatee Zathul³⁹, A. Kheirandish^{33, 34}, H. Kimku⁵³, J. Kiryluk⁵⁵, C. Klein²⁵, S. R. Klein^{6, 7}, Y. Kobayashi¹⁵, A. Kochocki²³, R. Koirala⁴³, H. Kolanoski⁸, T. Kontrimas²⁶, L. Köpke⁴⁰, C. Kopfer²⁵, D. J. Koskinen²¹, P. Koundal⁴³, M. Kowalski^{8, 63}, T. Kozynets²¹, N. Krieger⁹, J. Krishnamoorthi^{39, a}, T. Krishnan¹³, K. Kruiswijk³⁶, E. Krupczak²³, A. Kumar⁶³, E. Kun⁹, N. Kurahashi⁴⁸, N. Lad⁶³, C. Lagunas Gualda²⁶, L. Lallement Arnaud¹⁰, M. Lamoureux³⁶, M. J. Larson¹⁸, F. Lauber⁶², J. P. Lazar³⁶, K. Leonard DeHolton⁶⁰, A. Leszczyńska⁴³, J. Liao⁴, C. Lin⁴³, Y. T. Liu⁶⁰, M. Liubarska²⁴, C. Love⁴⁸, L. Lu³⁹, F. Lucarelli²⁷, W. Luszcza^{19, 20}, Y. Lyu^{6, 7}, J. Madsen³⁹, E. Magnus¹¹, K. B. M. Mahn²³, Y. Makino³⁹, E. Manao²⁶, S. Mancina^{47, e}, A. Mand³⁹, I. C. Mariş¹⁰, S. Marka⁴⁵, Z. Marka⁴⁵, L. Marten¹, I. Martinez-Soler¹³, R. Maruyama⁴⁴, J. Mauro³⁶, F. Mayhew²³, F. McNally³⁷, J. V. Mead²¹, K. Meagher³⁹, S. Mechbal⁶³, A. Medina²⁰, M. Meier¹⁵, Y. Merckx¹¹, L. Merten⁹, J. Mitchell⁵, L. Molchany⁴⁹, T. Montaruli²⁷, R. W. Moore²⁴, Y. Morii¹⁵, A. Mosbrugger²⁵, M. Moulai³⁹, D. Mousadi⁶³, E. Moyaux³⁶, T. Mukherjee³⁰, R. Naab⁶³, M. Nakos³⁹, U. Naumann⁶², J. Necker⁶³, L. Neste⁵⁴, M. Neumann⁴², H. Niederhausen²³, M. U. Nisa²³, K. Noda¹⁵, A. Noell¹, A. Novikov⁴³, A. Obertacke Pollmann¹⁵, V. O'Dell³⁹, A. Olivas¹⁸, R. Orsoe²⁶, J. Osborn³⁹, E. O'Sullivan⁶¹, V. Palusova⁴⁰, H. Pandya⁴³, A. Parenti¹⁰, N. Park³², V. Parrish²³, E. N. Paudel⁵⁸, L. Paul⁴⁹, C. Pérez de los Heros⁶¹, T. Pernice⁶³, J. Peterson³⁹, M. Plum⁴⁹, A. Pontén⁶¹, V. Poojyam⁵⁸, Y. Popovych⁴⁰, M. Prado Rodriguez³⁹, B. Pries²³, R. Procter-Murphy¹⁸, G. T. Przybylski⁷, L. Pyras⁵², C. Raab³⁶, J. Rack-Helleis⁴⁰, N. Rad⁶³, M. Ravn⁶¹, K. Rawlins³, Z. Rechav³⁹, A. Rehman⁴³, I. Reistoffer⁴⁹, E. Resconi²⁶, S. Reusch⁶³, C. D. Rho⁵⁶, W. Rhode²², L. Ricca³⁶, B. Riedel³⁹, A. Rifaie⁶², E. J. Roberts², S. Robertson^{6, 7}, M. Rongen²⁵, A. Rosted¹⁵, C. Rott⁵², T. Ruhe²², L. Ruohan²⁶, D. Ryckbosch²⁸, J. Saffer³¹, D. Salazar-Gallegos²³, P. Sampathkumar³⁰, A. Sandrock⁶², G. Sanger-Johnson²³, M. Santander⁵⁸, S. Sarkar⁴⁶, J. Savelberg¹, M. Scarnera³⁶, P. Schaile²⁶, M. Schaufel¹, H. Schieler³⁰, S. Schindler²⁵, L. Schlickmann⁴⁰, B. Schlüter⁴², F. Schlüter¹⁰, N. Schmeisser⁶², T. Schmidt¹⁸, F. G. Schröder^{30, 43}, L. Schumacher²⁵, S. Schwirn¹, S. Sclafani¹⁸, D. Seckel⁴³, L. Seen³⁹, M. Seikh³⁵, S. Seunarine⁵⁰, P. A. Seville Myhr³⁶, R. Shah⁴⁸, S. Shefali³¹, N. Shimizu¹⁵, B. Skrzypek⁶, R. Snihur³⁹, J. Soedingrekso²², A. Sogaard²¹, D. Soldin⁵², P. Soldin¹, G. Sommani⁹, C. Spannfellner²⁶, G. M. Spiczak⁵⁰, C. Spiering⁶³, J. Stachurska²⁸, M. Stamatikos²⁰, T. Stanev⁴³, T. Stezelberger⁷, T. Stürwald⁶², T. Stüttard²¹, G. W. Sullivan¹⁸, I. Taboada⁴, S. Ter-Antonyan⁵, A. Terliuk²⁶, A. Thakuri⁴⁹, M. Thiesmeyer³⁹, W. G. Thompson¹³, J. Thwaites³⁹, S. Tilav⁴³, K. Tollefson²³, S. Toscano¹⁰, D. Tosi³⁹, A. Trettin⁶³, A. K. Upadhyay^{39, a}, K. Upshaw⁵, A. Vaidyanathan⁴¹, N. Valtonen-Mattila^{9, 61}, J. Valverde⁴¹, J. Vandenbroucke³⁹, T. van Eeden⁶³, N. van Eijndhoven¹¹, L. van Rootselaar²², J. van Santen⁶³, F. J. Vara Carbonell⁴², F. Varsi³¹, M. Venugopal³⁰, M. Vereecken³⁶, S. Vergara Carrasco¹⁷, S. Verpoest⁴³, D. Veske⁴⁵, A. Vijai¹⁸, J. Villarreal¹⁴, C. Walck⁵⁴, A. Wang⁴, E. Warrick⁵⁸, C. Weaver²³, P. Weigel¹⁴, A. Weindl³⁰, J. Weldert⁴⁰, A. Y. Wen¹³, C. Wendt³⁹, J. Werthebach²², M. Weyrauch³⁰, N. Whitehorn²³, C. H. Wiebusch¹, D. R. Williams⁵⁸, L. Witthaus²², M. Wolf²⁶, G. Wrede²⁵, X. W. Xu⁵, J. P. Yañez²⁴, Y. Yao³⁹, E. Yildizci³⁹, S. Yoshida¹⁵, R. Young³⁵, F. Yu¹³, S. Yu⁵², T. Yuan³⁹, A. Zegarelli⁹, S. Zhang²³, Z. Zhang⁵⁵, P. Zhelnin¹³, P. Zilberman³⁹

¹ III. Physikalisches Institut, RWTH Aachen University, D-52056 Aachen, Germany² Department of Physics, University of Adelaide, Adelaide, 5005, Australia³ Dept. of Physics and Astronomy, University of Alaska Anchorage, 3211 Providence Dr., Anchorage, AK 99508, USA⁴ School of Physics and Center for Relativistic Astrophysics, Georgia Institute of Technology, Atlanta, GA 30332, USA⁵ Dept. of Physics, Southern University, Baton Rouge, LA 70813, USA⁶ Dept. of Physics, University of California, Berkeley, CA 94720, USA⁷ Lawrence Berkeley National Laboratory, Berkeley, CA 94720, USA⁸ Institut für Physik, Humboldt-Universität zu Berlin, D-12489 Berlin, Germany⁹ Fakultät für Physik & Astronomie, Ruhr-Universität Bochum, D-44780 Bochum, Germany¹⁰ Université Libre de Bruxelles, Science Faculty CP230, B-1050 Brussels, Belgium

- ¹¹ Vrije Universiteit Brussel (VUB), Dienst ELEM, B-1050 Brussels, Belgium
- ¹² Dept. of Physics, Simon Fraser University, Burnaby, BC V5A 1S6, Canada
- ¹³ Department of Physics and Laboratory for Particle Physics and Cosmology, Harvard University, Cambridge, MA 02138, USA
- ¹⁴ Dept. of Physics, Massachusetts Institute of Technology, Cambridge, MA 02139, USA
- ¹⁵ Dept. of Physics and The International Center for Hadron Astrophysics, Chiba University, Chiba 263-8522, Japan
- ¹⁶ Department of Physics, Loyola University Chicago, Chicago, IL 60660, USA
- ¹⁷ Dept. of Physics and Astronomy, University of Canterbury, Private Bag 4800, Christchurch, New Zealand
- ¹⁸ Dept. of Physics, University of Maryland, College Park, MD 20742, USA
- ¹⁹ Dept. of Astronomy, Ohio State University, Columbus, OH 43210, USA
- ²⁰ Dept. of Physics and Center for Cosmology and Astro-Particle Physics, Ohio State University, Columbus, OH 43210, USA
- ²¹ Niels Bohr Institute, University of Copenhagen, DK-2100 Copenhagen, Denmark
- ²² Dept. of Physics, TU Dortmund University, D-44221 Dortmund, Germany
- ²³ Dept. of Physics and Astronomy, Michigan State University, East Lansing, MI 48824, USA
- ²⁴ Dept. of Physics, University of Alberta, Edmonton, Alberta, T6G 2E1, Canada
- ²⁵ Erlangen Centre for Astroparticle Physics, Friedrich-Alexander-Universität Erlangen-Nürnberg, D-91058 Erlangen, Germany
- ²⁶ Physik-department, Technische Universität München, D-85748 Garching, Germany
- ²⁷ Département de physique nucléaire et corpusculaire, Université de Genève, CH-1211 Genève, Switzerland
- ²⁸ Dept. of Physics and Astronomy, University of Gent, B-9000 Gent, Belgium
- ²⁹ Dept. of Physics and Astronomy, University of California, Irvine, CA 92697, USA
- ³⁰ Karlsruhe Institute of Technology, Institute for Astroparticle Physics, D-76021 Karlsruhe, Germany
- ³¹ Karlsruhe Institute of Technology, Institute of Experimental Particle Physics, D-76021 Karlsruhe, Germany
- ³² Dept. of Physics, Engineering Physics, and Astronomy, Queen's University, Kingston, ON K7L 3N6, Canada
- ³³ Department of Physics & Astronomy, University of Nevada, Las Vegas, NV 89154, USA
- ³⁴ Nevada Center for Astrophysics, University of Nevada, Las Vegas, NV 89154, USA
- ³⁵ Dept. of Physics and Astronomy, University of Kansas, Lawrence, KS 66045, USA
- ³⁶ Centre for Cosmology, Particle Physics and Phenomenology - CP3, Université catholique de Louvain, Louvain-la-Neuve, Belgium
- ³⁷ Department of Physics, Mercer University, Macon, GA 31207-0001, USA
- ³⁸ Dept. of Astronomy, University of Wisconsin—Madison, Madison, WI 53706, USA
- ³⁹ Dept. of Physics and Wisconsin IceCube Particle Astrophysics Center, University of Wisconsin—Madison, Madison, WI 53706, USA
- ⁴⁰ Institute of Physics, University of Mainz, Staudinger Weg 7, D-55099 Mainz, Germany
- ⁴¹ Department of Physics, Marquette University, Milwaukee, WI 53201, USA
- ⁴² Institut für Kernphysik, Universität Münster, D-48149 Münster, Germany
- ⁴³ Bartol Research Institute and Dept. of Physics and Astronomy, University of Delaware, Newark, DE 19716, USA
- ⁴⁴ Dept. of Physics, Yale University, New Haven, CT 06520, USA
- ⁴⁵ Columbia Astrophysics and Nevis Laboratories, Columbia University, New York, NY 10027, USA
- ⁴⁶ Dept. of Physics, University of Oxford, Parks Road, Oxford OX1 3PU, United Kingdom
- ⁴⁷ Dipartimento di Fisica e Astronomia Galileo Galilei, Università Degli Studi di Padova, I-35122 Padova PD, Italy
- ⁴⁸ Dept. of Physics, Drexel University, 3141 Chestnut Street, Philadelphia, PA 19104, USA
- ⁴⁹ Physics Department, South Dakota School of Mines and Technology, Rapid City, SD 57701, USA
- ⁵⁰ Dept. of Physics, University of Wisconsin, River Falls, WI 54022, USA
- ⁵¹ Dept. of Physics and Astronomy, University of Rochester, Rochester, NY 14627, USA
- ⁵² Department of Physics and Astronomy, University of Utah, Salt Lake City, UT 84112, USA
- ⁵³ Dept. of Physics, Chung-Ang University, Seoul 06974, Republic of Korea
- ⁵⁴ Oskar Klein Centre and Dept. of Physics, Stockholm University, SE-10691 Stockholm, Sweden
- ⁵⁵ Dept. of Physics and Astronomy, Stony Brook University, Stony Brook, NY 11794-3800, USA
- ⁵⁶ Dept. of Physics, Sungkyunkwan University, Suwon 16419, Republic of Korea
- ⁵⁷ Institute of Physics, Academia Sinica, Taipei, 11529, Taiwan
- ⁵⁸ Dept. of Physics and Astronomy, University of Alabama, Tuscaloosa, AL 35487, USA
- ⁵⁹ Dept. of Astronomy and Astrophysics, Pennsylvania State University, University Park, PA 16802, USA
- ⁶⁰ Dept. of Physics, Pennsylvania State University, University Park, PA 16802, USA
- ⁶¹ Dept. of Physics and Astronomy, Uppsala University, Box 516, SE-75120 Uppsala, Sweden
- ⁶² Dept. of Physics, University of Wuppertal, D-42119 Wuppertal, Germany
- ⁶³ Deutsches Elektronen-Synchrotron DESY, Platanenallee 6, D-15738 Zeuthen, Germany
- ^a also at Institute of Physics, Sachivalaya Marg, Sainik School Post, Bhubaneswar 751005, India
- ^b also at Department of Space, Earth and Environment, Chalmers University of Technology, 412 96 Gothenburg, Sweden
- ^c also at INFN Padova, I-35131 Padova, Italy
- ^d also at Earthquake Research Institute, University of Tokyo, Bunkyo, Tokyo 113-0032, Japan
- ^e now at INFN Padova, I-35131 Padova, Italy

Acknowledgments

The authors gratefully acknowledge the support from the following agencies and institutions: USA – U.S. National Science Foundation-Office of Polar Programs, U.S. National Science Foundation-Physics Division, U.S. National Science Foundation-EPSCoR, U.S. National Science Foundation-Office of Advanced Cyberinfrastructure, Wisconsin Alumni Research Foundation, Center for High Throughput Computing (CHTC) at the University of Wisconsin–Madison, Open Science Grid (OSG), Partnership to Advance Throughput Computing (PATH), Advanced Cyberinfrastructure Coordination Ecosystem: Services & Support (ACCESS), Frontera and Ranch computing project at the Texas Advanced Computing Center, U.S. Department of Energy-National Energy Research Scientific Computing Center, Particle astrophysics research computing center at the University of Maryland, Institute for Cyber-Enabled Research at Michigan State University, Astroparticle physics computational facility at Marquette University, NVIDIA Corporation, and Google Cloud Platform; Belgium – Funds for Scientific Research (FRS-FNRS and FWO), FWO Odysseus and Big Science programmes, and Belgian Federal Science Policy Office (Belspo); Germany – Bundesministerium für Forschung, Technologie und Raumfahrt (BMFT), Deutsche Forschungsgemeinschaft (DFG), Helmholtz Alliance for Astroparticle Physics (HAP), Initiative and Networking Fund of the Helmholtz Association, Deutsches Elektronen Synchrotron (DESY), and High Performance Computing cluster of the RWTH Aachen; Sweden – Swedish Research Council, Swedish Polar Research Secretariat, Swedish National Infrastructure for Computing (SNIC), and Knut and Alice Wallenberg Foundation; European Union – EGI Advanced Computing for research; Australia – Australian Research Council; Canada – Natural Sciences and Engineering Research Council of Canada, Calcul Québec, Compute Ontario, Canada Foundation for Innovation, WestGrid, and Digital Research Alliance of Canada; Denmark – Villum Fonden, Carlsberg Foundation, and European Commission; New Zealand – Marsden Fund; Japan – Japan Society for Promotion of Science (JSPS) and Institute for Global Prominent Research (IGPR) of Chiba University; Korea – National Research Foundation of Korea (NRF); Switzerland – Swiss National Science Foundation (SNSF).